Journal of Advanced Research xxx (xxxx) 1–10

Contents lists available at ScienceDirect

Journal of Advanced Research

journal homepage: www.elsevier.com

Activation of mitochondrial aldehyde dehydrogenase 2 promotes hair growth in human hair follicles

Seunghee Lee [a, b, c, d], Jungyoon Ohn [a, b, c], Bo Mi Kang [a, b, c], Sungjoo Tommy Hwang [e], Ohsang Kwon [a, b, c, d, *]

[a] Department of Dermatology, Seoul National University College of Medicine, Seoul 03080, South Korea
[b] Laboratory of Cutaneous Aging and Hair Research, Biomedical Research Institute, Seoul National University Hospital, Seoul 03080, South Korea
[c] Institute of Human-Environment Interface Biology, Medical Research Center, Seoul National University, Seoul 03080, South Korea
[d] Department of Biomedical Sciences, Seoul National University College of Medicine, Seoul 03080, South Korea
[e] Dr. Hwang's Hair-Hair Clinic, Seoul 06035, South Korea

ARTICLE INFO

Article history:
Received 9 April 2023
Received in revised form 6 November 2023
Accepted 12 November 2023

Keywords:
Aldehyde dehydrogenase 2
Hair growth
Oxidative stress
Hair follicle
Outer root sheath
β-catenin

ABSTRACT

Introduction: Hair loss is a common phenomenon associated with various environmental and genetic factors. Mitochondrial dysfunction-induced oxidative stress has been recognized as a crucial determinant of hair follicle (HF) biology. Aldehyde dehydrogenase 2 (ALDH2) mitigates oxidative stress by detoxifying acetaldehyde. This study investigated the potential role of ALDH2 modulation in HF function and hair growth promotion.
Objectives: To evaluate the effects of ALDH2 activation on oxidative stress in HFs and hair growth promotion.
Methods: The modulatory role of ALDH2 on HFs was investigated using an ALDH2 activator. ALDH2 expression in human HFs was evaluated through *in vitro* immunofluorescence staining. *Ex vivo* HF organ culture was employed to assess hair shaft elongation, while the fluorescence probe 2′,7′- dichlorodihydrofluorescein diacetate was utilized to detect reactive oxygen species (ROS). An *in vivo* mouse model was used to determine whether ALDH2 activation induces anagen.
Results: During the anagen phase, ALDH2 showed significantly higher intensity than that in the telogen phase, and its expression was primarily localized along the outer layer of HFs. ALDH2 activation promoted anagen phase induction by reducing ROS levels and enhancing reactive aldehyde clearance, which indicated that ALDH2 functions as a ROS scavenger within HFs. Moreover, ALDH2 activation upregulated Akt/GSK 3β/β-catenin signaling in HFs.
Conclusions: Our findings highlight the hair growth promotion effects of ALDH2 activation in HFs and its potential as a promising therapeutic approach for promoting anagen induction.

Introduction

A multitude of environmental and genetic factors contribute to the global phenomenon of hair loss [1–3]. Hair follicles (HFs) undergo a cyclical process of growth, regression, and rest, known as the anagen, catagen, and telogen phases, respectively [4]. Particularly, the anagen phase, responsible for hair growth, necessitates an ample energy supply facilitated by proficient mitochondrial function [5,6]. Adequate mitochondrial energy supply is crucial for successful transition from the resting phase to the growth phase [7,8]. Furthermore, cell division rates during the anagen phase are high, which is correlated with increased protein synthesis owing to HF formation [9,10]. To sustain this rapid proliferation and maintain a normal hair cycle, substantial energy and metabolic expenditures are indispensable. Nonetheless, mitochondrial dysfunction may interrupt the regular hair cycle, leading to hair loss [11].

Hair loss is significantly associated with the oxidative stress induced by impaired mitochondrial function, which triggers the production of excess reactive oxygen species (ROS) [12]. Elevation in intracellular ROS levels in HFs leads to oxidative stress, resulting in hair loss upon entering the catagen phase [13]. Oxidative stress is a cytotoxic event that downregulates the activity of dermal papilla cells (DPCs). Moreover, it inhibits the activation of HF-morphogenesis-related proteins, thereby suppressing hair growth and ultimately causing hair loss. This phenomenon is of great significance in the study of hair-related disorders [14,15].

Among the family of aldehyde dehydrogenases, aldehyde dehydrogenase 2 (ALDH2) attenuates oxidative stress and sustains cellular homeostasis [16]. Although its exact mechanism of action in lowering

* Corresponding author at: Department of Dermatology, Seoul National University College of Medicine, South Korea.
E-mail address: oskwon@snu.ac.kr (O. Kwon).

https://doi.org/10.1016/j.jare.2023.11.014
2090-1232/© 20XX

oxidative stress and its impact on hair growth remain elusive, ALDH2 regulates aldehyde metabolism by targeting cytotoxic aldehydes and eliminating 4-hydroxynonenal (4-HNE) and malondialdehyde (MDA) [17]. Recent studies have highlighted the potential of ALDH2, a regulator of oxidative stress and redox signaling pathways, as a therapeutic target for diseases owing to its ability to reduce 4-HNE production and metabolize toxic substances [18]. Furthermore, ALDH2 activation leads to the inhibition of oxidative stress during hepatic ischemia/reperfusion injury and accelerates the degradation of reactive aldehyde adducts, resulting in cell death [19].

Taken together, we aimed to evaluate the effects of ALDH2 activation on human HFs and its potential to promote hair growth. We hypothesized that modulation of ALDH2 would eliminate aldehyde adducts in HFs, thereby stimulating hair growth. We conducted experiments utilizing human hair tissues, outer root sheath cells (ORSCs), and DPCs to determine whether ALDH2 activation accelerates hair growth. Our findings demonstrate the role of ALDH2 activation in augmenting hair growth. This process aligns with the enhancement of β-catenin accumulation, serving as a key signaling mechanism. Moreover, our results provide novel insights into the impact of ALDH2 activation on HFs and highlight its potential as a viable therapeutic approach for anagen phase induction in hair growth cycles.

Materials and Methods

Ethics statement

The human study was approved by the Institutional Review Board of Seoul National University Hospital (2209–021-1356) and followed ethical guidelines. Animal research was approved by the Institutional Animal Care and Use Committee of Seoul National University Hospital (20-0166-S1A1).

Cell culture of ORSCs and DPCs

The isolation of human ORSCs was conducted according to a previous study [20,21]. To prevent contamination with extraneous follicular cell types, human ORSCs were cultured by trimming away both the infundibular sections down to the sebaceous gland and the bulbar part of the HFs [22,23]. The trimmed HFs were then incubated with Dulbecco's modified Eagle's medium (DMEM; Welgene, Daegu, Republic of Korea) containing 20% fetal bovine serum (FBS). On the 2nd day of culturing, keratinocyte growth medium (Lonza, Basel, Switzerland), supplemented with hydrocortisone, transferrin, epinephrine, gentamicin, bovine pituitary exact, human epidermal growth factor and insulin was added, and the cells were maintained at 37 ˚C in a 5% CO_2 atmosphere. DPCs were prepared by dissecting the bulb region to isolate candlelight-shaped DPCs [24,25]. The DPCs were incubated in DMEM containing 20% FBS and an antimicrobial solution (Gibco BRL, Gaithersburg, MD, USA). Following a 14-day period of adhesion to the culture plate, the medium was replaced every two days with DMEM containing 10% FBS, and the cells were preserved at 37 ˚C in a 5% CO_2 atmosphere.

Measurement of ALDH2 activity

Human ORSCs were cultured in cell culture plates exposed to Alda-1, which activates ALDH2, and a control solution in a medium without serum. Subsequently, the samples were harvested and centrifuged at 500 × *g* to isolate cellular pellets. These pellets were resuspended in an extraction buffer and incubated on ice for 20 min. ALDH2 enzyme activity was measured and analyzed using an ALDH2 assay kit (Abcam, Cambridge, UK) according to the manufacturer's instructions. As part of the ALDH2-catalyzed reaction, nicotinamide adenine dinucleotide production was measured. A fluorescence microplate reader (VersaMax, Molecular Devices Corporation, San Jose, CA, USA) was used to assess ALDH2 activity at an absorbance of 450 nm.

Isolation of human scalp tissue and HF organ culture

Human scalp samples (1.5 cm × 1.0 cm) from the occipital region were obtained from healthy volunteers and cultured according to a previously described protocol [26,27]. Each HF was trimmed at the sebaceous duct level using a stereomicroscope (Olympus, Tokyo, Japan) and incubated in Williams E medium (Gibco BRL, Gaithersburg, MD, USA), containing l-glutamine and insulin as well as penicillin and hydrocortisone, for 6 days. The HFs were obtained from five independent donors, with eight HFs per group, totaling 40 HFs. Subsequently, these HFs were treated with Alda-1 in the culture medium at concentrations of 5, 25, and 50 μM.

Cell viability assays

DPCs and ORSCs were prepared in a medium devoid of serum. After a day, the cells were incubated with 25, 50, and 100 μM Alda-1 and 1 μM Minoxidil for 48 h. The viability test was carried out by adding the cell counting Kit-8 solution (Dojindo, Kumamoto, Japan) to wells and incubating the samples at 37 ˚C. Then, a plate reader was used to record the absorbance at 450 nm. The relative viability was calculated by normalizing to the control group. The employed assay utilized a water-soluble tetrazolium salt for the quantification of viable cells; viability was indicated by the formation of an orange formazan dye upon bioreduction.

ROS scavenging

The levels of ROS were determined using the 2′, 7′- dichlorodihydrofluorescein diacetate (H_2DCFDA) fluorescence probe. Subsequently, the ORSCs and DPCs treated with Alda-1 or vehicle were rinsed with PBS and incubated with H_2DCFDA at 37 ˚C for 30 min in the dark. Subsequently, green fluorescence images were acquired using fluorescence microscopy (Nikon, Tokyo, Japan). Brightfield images of ORSCs and DPCs were obtained via stereotype microscopy (Olympus, Tokyo, Japan). Flow cytometry analysis was employed to detect and measure H_2DCFDA levels within the ORSCs. The data obtained from flow cytometry experiments were analyzed using the FlowJo™ software and then normalized.

Oxygen consumption rate (OCR)

OCR measurement was conducted using a previously described method [28]. ORSCs were seeded in a Seahorse XF24 and incubated overnight. Following the incubation, the previous medium was replaced with a serum-free medium and ORSCs were treated with the vehicle and 50 μM Alda-1. Seahorse cartridges were then used for conducting assays through ports. The following compounds were added: oligomycin, a compound that inhibits adenosine triphosphate (ATP) synthase; carbonyl cyanide p-(trifluoromethoxy) phenylhydrazone (FCCP), a compound that uncouples oxidative phosphorylation; rotenone, a compound that inhibits the mitochondrial respiratory chain at complex I; antimycin A, a compound that inhibits the mitochondrial respiratory chain responsible for ATP generation via oxidative phosphorylation.

ATP production rate

Mitochondrial and glycolytic ATP production rates were evaluated using the Seahorse XF Real-Time ATP Rate Assay (Agilent Technologies, Santa Clara, CA, USA) according to the manufacturer's protocol. ORSCs were seeded into specialized XF cell culture microplates de-

signed for the assay. Following a 24 h starvation period, ORSCs were exposed to either the vehicle or 50 μM Alda-1 in serum-free medium for an additional 24 h. Subsequently, the microplate was incubated at 37 ˚C in a non-CO_2 incubator for 60 min. Using the Seahorse XFe96 analyzer, the ATP production rates were then measured and normalized to cell number.

Western blot analysis

To lyse the human ORSCs and DPCs, RIPA buffer (Millipore, Merck, Burlington, MA, USA) was employed. The proteins were separated via sodium dodecyl-sulfate (SDS)-polyacrylamide gel electrophoresis, which uses an SDS detergent and polyacrylamide gel matrix to separate proteins based on their size. Subsequently, the proteins were electrotransferred onto an Amersham membrane and probed with primary antibodies to enable protein detection. Commercially available primary antibodies, including β-actin diluted at 1:5,000, phospho-Akt, Akt, phospho-GSK 3β, GSK 3β, non-phospho β-catenin, and β-catenin, from Cell Signaling Technology (Danvers, MA, USA) were employed. These antibodies were utilized at a dilution of 1:1,000. After incubation with antibodies, the membranes were treated with immunoglobulin G (IgG) antibodies (GeneTex, Irvine, CA, USA). The detection of the binding events between primary antibodies and their respective targets was achieved using a chemiluminescent substrate (Thermo Fisher Scientific), and signal detection was carried out using Amersham imager 680 systems (GE Healthcare, Chicago, IL, USA). Subsequently, the captured images were analyzed for quantification.

Human growth factor detection

The Human Growth Factor Antibody kit (Raybiotech, Peachtree Corners, GA, USA) was employed to identify specific hair growth factors in the process under investigation. DPCs were treated with serum-free DMEM containing the control or 50 μM Alda-1. Following treatment, the culture media were harvested, centrifuged at 1800 rpm for 10 min, and then subjected to filtration through a 0.22-μm syringe filter. The resultant filtrate was subjected to an additional centrifugation step using Vivaspin (Sartorius, Göttingen, Germany). Membranes were subjected to an overnight incubation at 4 ˚C in conditional media derived from DPCs and treated with either the vehicle or Alda-1 [29]. Subsequently, the immunoreactivity was captured using Amersham imager 680 systems (GE Healthcare).

Anagen induction study

The *in vivo* assessment of anagen induction was performed as described previously [4]. Briefly, female C57BL/6 mice (8-week-old) in the telogen phase were shaved, and topical application of either vehicle, 0.5 and 3 mM Alda-1 solutions, or 2% Minoxidil was administered weekly. A previously reported method was utilized with minor modifications to evaluate the skin thickness and anagen induction scores, wherein the telogen phase was assigned a score of 1 and anagen I–VI were assigned scores of 2–7, respectively.

Immunofluorescence (IF) staining

Human HFs embedded in paraffin and mouse dorsal cutaneous tissue were sectioned at thicknesses of 7 and 4 μm, respectively. The DPCs and ORSCs were cultured on culture slides (SPL Life Sciences, Pocheon, Korea) and fixed in 4% paraformaldehyde. To perform IF staining, specific primary antibodies were applied to the tissues and cells overnight at 4 ˚C. The following antibodies were prepared with the diluent reagent (Invitrogen, Thermo Fisher Scientific): ALDH2 (1:200; Thermo Fisher Scientific), voltage-dependent anion-selective channel (VDAC; 1:200; Thermo Fisher Scientific), Ki-67 (1:200; Dako, Agilent Technologies), versican (1:200; Abcam), and β-catenin (1:200; Cell Signaling Technology). Following PBS washing, the slides were subjected to incubation with secondary antibodies, which were either anti-rabbit or mouse IgG antibodies conjugated with Alexa Fluor 488 (Invitrogen) or anti-rabbit IgG antibodies conjugated with Alexa Fluor 594 (Invitrogen) at a dilution of 1:200. In addition, 4′,6-diamidino-2-phenylindole (DAPI; Invitrogen) was employed for staining the cell nuclei at a ratio of 1:1,000.

Statistical analysis

Data are presented as mean accompanied by the standard error of the mean (SEM) to facilitate improved comprehension and precision. Statistical analyses were conducted using the GraphPad Prism 8 software (GraphPad Software, Boston, MA, USA). Student's *t*-test and two-tailed tests were executed, and the threshold for significance was established at $P < 0.05$. The animals and samples were randomly assigned to experimental groups. Data obtained from animal experiments were analyzed by researchers who were unaware of the experimental conditions (blinded analysis).

Results

ALDH2 expression in human HFs

Immunostaining of HFs was conducted to evaluate the variation in ALDH2 expression levels from anagen to telogen. Briefly, ALDH2 activity was investigated using an ALDH2 antibody co-stained with VDAC as a mitochondrial marker. ALDH2 was expressed in human HFs with a remarkably higher intensity in the outer root sheath (ORS) than in other regions (Fig. 1A). Conversely, the expression of ALDH2 was reduced in the hair matrix, inner root sheath (IRS), and dermal papilla compared with that in the ORS region. There was a discernible augmentation in ALDH2 levels in HFs during the anagen phase, particularly in the ORS (Supplementary Fig. 1A, 1B). Together with the results presented in Fig. 1A, these findings confirmed that ALDH2 expression was similar in the distal and proximal follicle bulb ORS. Quantification of ALDH2 fluorescence intensity further confirmed its significantly augmented expression in the anagen phase relative to that in the telogen phase (Fig. 1B).

To further investigate the role of ALDH2 in human HFs, we assessed its activity at the cellular level in ORSCs and DPCs using IF staining (Fig. 1C, Supplementary Fig. 1D). As depicted in Fig. 1A and B, ALDH2 expression was primarily localized in ORSCs. Moreover, the relative ALDH2 protein levels were significantly higher in ORSCs than in DPCs (Supplementary Fig. 1C).

Effects of ALDH2 activation on human ORSCs and hair shaft elongation

To explore the impact of Alda-1 on HFs, we conducted an assessment of ALDH2 enzymatic activity in ORSCs. A significant increase was observed in ALDH2 activity in ORSCs after Alda-1 treatment (Fig. 2A), indicating that Alda-1 functions as an ALDH2 activator in HFs, thereby modulating ALDH2 expression. Furthermore, to identify the optimal Alda-1 concentration for stimulating ALDH2 activity in HFs, we evaluated ORSC viability after treatment with various concentrations of Alda-1 for up to 48 h. Cell proliferation was elevated in a dose-dependent manner upon treatment with 5, 25, and 50 μM Alda-1, whereas it was reduced with 100 μM Alda-1 treatment (Fig. 2B). Upon treatment with 50 μM Alda-1, cell viability significantly increased after 24 and 48 h. Based on these results, we selected 5, 25, and 50 μM Alda-1 concentrations for further investigation.

To assess whether ALDH2 activation promotes hair shaft elongation, we performed *ex vivo* HF organ cultures. Hair shaft elongation length was measured after treatment with 5, 25, and 50 μM Alda-1 for up to 6 days. A dose-dependent elongation in hair shaft length was noted fol-

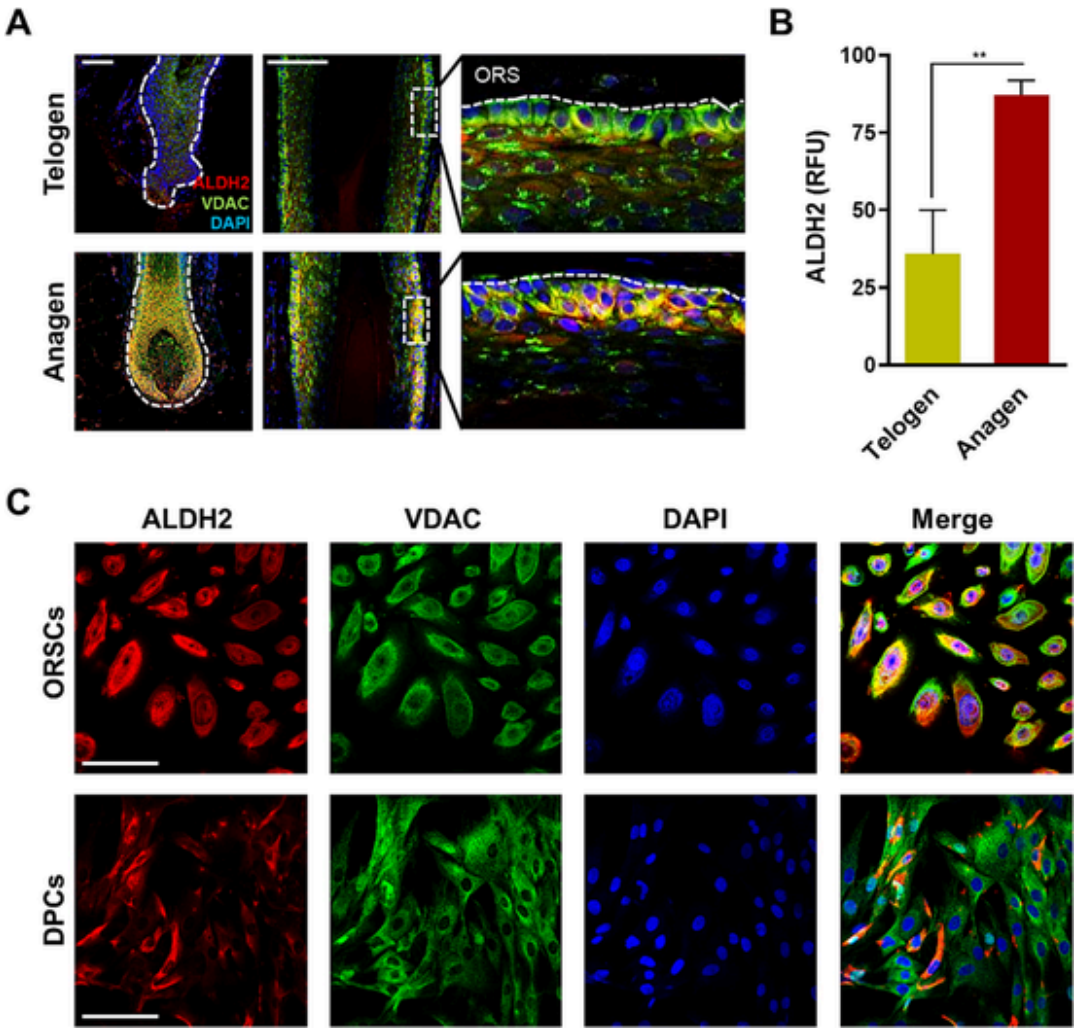

Fig. 1. ALDH2 expression in human HFs. (A) Immunostaining analysis revealed distinct ALDH2 localization predominantly in the outermost layer of HFs. The delineated region (dashed line) represents the ORS; scale bar = 100 μm (Left and center panel). The right panel is the designated part of center panel magnified 5 × and then rotated anticlockwise. (B) Relative fluorescence unit (RFU) calculated using the Image J software. In the anagen phase, there was a higher ALDH2 fluorescence intensity than that during the telogen phase (n = 3 technical replicates in ORS region of HFs/group); statistical comparison was performed using an unpaired t-test; Data are presented as mean ± SEM; **, $P < 0.01$. (C) Higher ALDH2 expression levels in ORSCs than in DPCs are shown; scale bar = 50 μm. ALDH2: aldehyde dehydrogenase 2, VDAC: voltage-dependent anion-selective channel, DAPI: 4′,6-diamidino-2-phenylindole, ORS: outer root sheath, ORSCs: outer root sheath cells, DPCs: dermal papilla cells, HF: hair follicle.

lowing Alda-1 treatment (Fig. 2C). Furthermore, increasing the concentration of Alda-1 significantly improved the growth rate of the hair shaft.

Ki-67 is a widely used cell proliferation marker for the quantification of cellular expression levels during the anagen phase [26,30]. To evaluate cell proliferation, we performed Ki-67 IF staining (Fig. 2D). The number of cells exhibiting positive Ki-67 staining in the matrix region was increased in the Alda-1-treated group. Specifically, the groups treated with 25 and 50 μM Alda-1 exhibited a significant increase compared to the control group. Upon treatment with Alda-1 at 50 μM, a marked increase in proliferation levels was observed relative to that in the lower concentration groups. The proliferation levels in the control group were 12.19 ± 0.64%, whereas in the 50 μM Alda-1-treated group, they increased to 52.96 ± 3.29% (Fig. 2E). These findings suggest that the Alda-1-mediated activation of ALDH2 promotes hair growth *ex vivo*.

ALDH2 activation in ORSCs induced ROS scavenging

The cell permeating H_2DCFDA is a widely employed probe for measuring ROS expression levels [31]. To determine whether ALDH2 acts as a ROS scavenger in HFs, ROS levels were evaluated in ORSCs using H_2DCFDA after Alda-1 treatment. The unstained group was also evaluated to confirm the effects of H_2DCFDA on ROS expression levels. The results indicated that ROS levels were remarkably upregulated in each group after hydrogen peroxide (H_2O_2) treatment. In the control group, peak levels of ROS were observed. After treatment with 5, 25, and 50 μM Alda-1, a dose-dependent reduction in ROS levels was observed. There was no difference in the cellular form, but the number of H_2DCFDA-stained cells decreased in the presence of ROS (Fig. 3A). Moreover, in DPCs, which are sensitive to oxidative stress, H_2DCFDA fluorescence was attenuated in an Alda-1 dose-dependent manner, further corroborating the suppression of ROS levels (Supplementary Fig. 2). ROS level reduction in ORSCs was further confirmed using flow cytometry. The control group treated with H_2O_2 and H_2DCFDA, in the rightmost position, had the highest level of ROS production. H_2DCFDA displayed a leftward shift in response to treatment with increasing con-

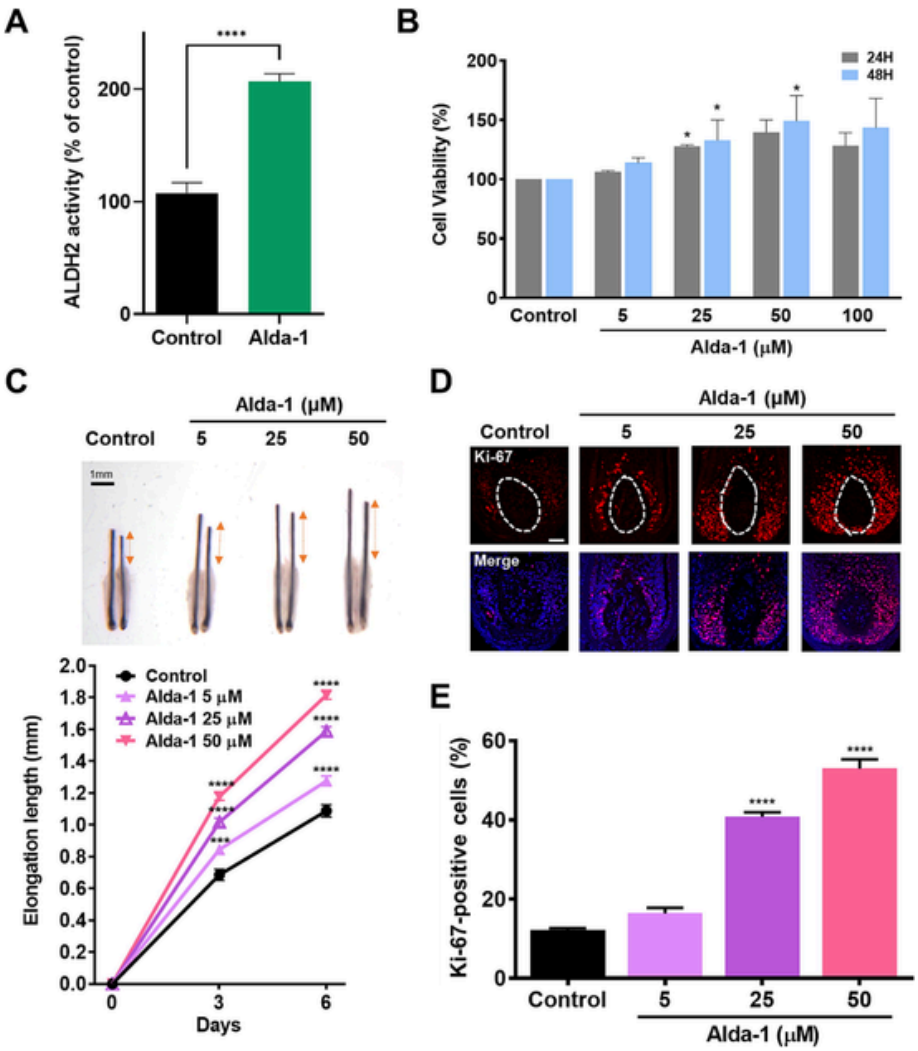

Fig. 2. Alda-1 promotes ALDH2 activation in human ORSCs and enhances hair shaft elongation. (A) Alda-1 treatment upregulated ALDH2 activation in ORSCs (n = 6 biological replicates/group); statistical comparison was performed using an unpaired t-test; Data are presented as mean ± SEM; ****, $P < 0.0001$. (B) Cell viability was higher in 25 and 50 μM Alda-1-treated ORSCs than in the vehicle-treated control ORSCs. Statistical significance determined using a two-way ANOVA with Dunnett's test compared with the control group. *, $P < 0.05$ (C) On day 6 of *ex vivo* organ culture, Alda-1 treatment significantly increased human hair shaft elongation; scale bar = 1 mm (n = 40 HFs in total, with 8 HFs/group from five independent donors); Statistical significance determined using a two-way ANOVA with Dunnett's test compared with the control group is shown as ***, $P < 0.001$; ****, $P < 0.0001$. (D) Immunofluorescence staining to evaluate Ki-67 expression in the human HF bulb region; scale bar = 100 μm. (E) Quantification of Ki-67 in the matrix region demonstrated a significant increase in Ki-67 upon Alda-1 treatment, with normalization to DAPI-stained cells (n = 5 HFs/group); statistical significance determined using a one-way ANOVA with Dunnett's test compared with the control group is shown as ****, $P < 0.0001$. Data are presented as mean ± SEM. ALDH2: aldehyde dehydrogenase 2, ORSCs: outer root sheath cells, HF: hair follicle, DAPI: 4′,6-diamidino-2-phenylindole.

centrations of Alda-1 (5, 25, and 50 μM), which implied a dose-dependent reduction in ROS levels at the cellular level relative to the levels observed in untreated samples (Fig. 3B). ALDH2 activation in ORSCs resulted in a significant decrease in ROS levels compared with that in the untreated control group (Fig. 3C). This observation highlights the potential role of ALDH2 activation in mitigating oxidative stress and modulating cellular redox homeostasis.

The build-up of ROS, 4-HNE, and MDA aldehydes exacerbate cytotoxicity and oxidative stress. Moreover, Alda-1 enhances ALDH2-mediated detoxification of both 4-HNE and MDA [32]. Our results revealed a significant dose-dependent decrease in 4-HNE levels upon treatment with Alda-1. Likewise, MDA levels decreased post-treatment with Alda-1 (Fig. 3D), which suggested that Alda-1 scavenges ROS and aldehyde adducts in ORSCs, which are involved in hair loss.

ALDH2 activation in ORSCs enhanced mitochondrial oxidative phosphorylation

ALDH2 is essential for maintaining mitochondrial homeostasis and regulating mitochondrial respiration [33]. Therefore, we assumed that the activation of ALDH2 would increase the mitochondrial respiratory levels. The OCR was evaluated to determine the effect of Alda-1 treatment on the mitochondrial respiration rate in ORSCs. For the normalization of OCR, DAPI was used to quantify viable cells via image analysis (Fig. 4A). The number of ORSCs increased 24 h after Alda-1 treatment. The observed cell count in the control group was 6637.57 ± 774.73 cells, and ALDH2 activation significantly elevated this number to 8780.29 ± 551.10 cells (Fig. 4B). As expected, mitochondrial OCR was stimulated by Alda-1 treatment (Fig. 4C). Basal respiration was quantified by subtracting nonmitochondrial respiration. The findings demonstrated that ALDH2 activation significantly upregulated the basal cellular respiration (Fig. 4D). The maximum respiration

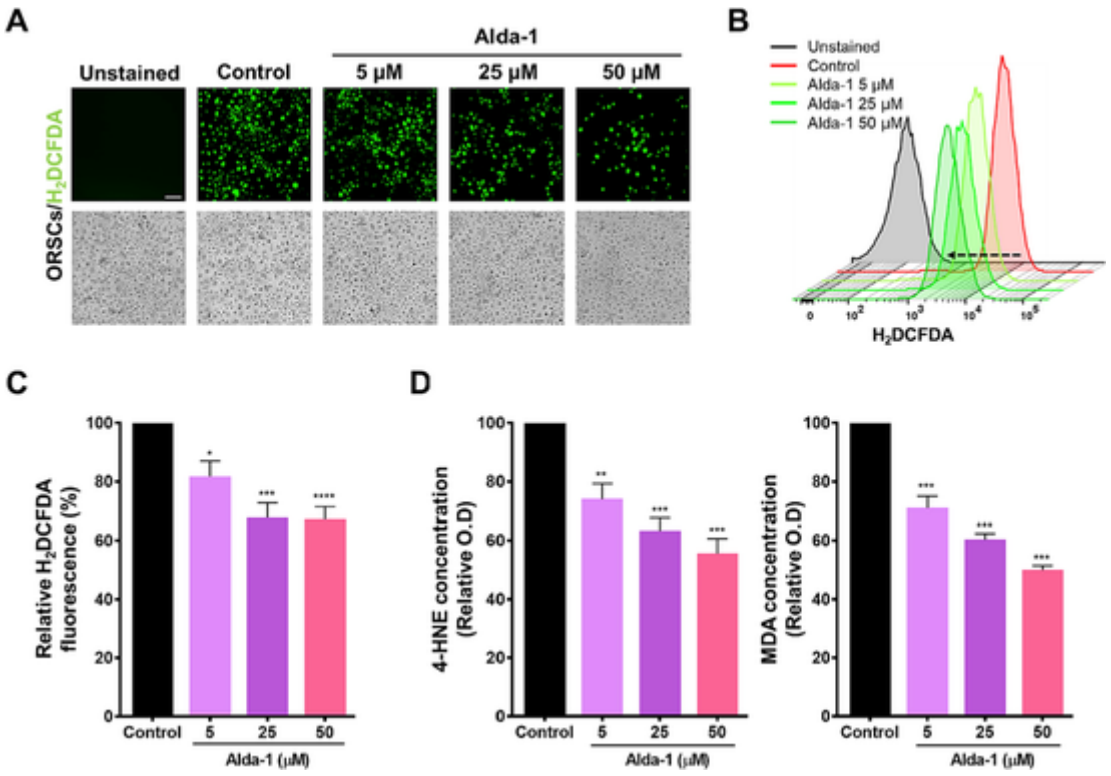

Fig. 3. ALDH2 activation induces ROS scavenging in ORSCs. (A) ORSCs treated with H_2O_2 to amplify ROS in each group and subsequently stained with H_2DCFDA are shown. The control group was treated with a vehicle, and the remaining ORSCs were treated with 5, 25, and 50 μM Alda-1; scale bar = 100 μm. (B) An Alda-1 dose-dependent reduction in H_2DCFDA fluorescence intensity was observed using flow cytometry analysis; left arrow indicates the reduction shift of H_2DCFDA. (C) Quantification of H_2DCFDA in flow cytometry analysis revealed that Alda-1 treatment downregulated ROS levels in ORSCs (n = 5 biological replicates/group). Statistical significance was assessed using a one-way ANOVA with Dunnett's test. *, $P < 0.05$; ***, $P < 0.001$; ****, $P < 0.0001$. (D) Following Alda-1 treatment of ORSCs, a dose-dependent reduction was observed in the levels of aldehyde adducts (n = 3/group). **, $P < 0.01$; ***, $P < 0.001$. In panels C and D, data are presented as mean ± SEM; statistical significance was assessed using a one-way ANOVA with Dunnett's test and compared with that in the control group. ORSCs: outer root sheath cells, H_2DCFDA: 2′,7′- dichlorodihydrofluorescein diacetate, O.D: optical density, ALDH2: aldehyde dehydrogenase 2, ROS: reactive oxygen species, H_2O_2: hydrogen peroxide, HNE: hydroxynonenal; MDA: malondialdehyde.

in ORSCs was measured after treatment with the mitochondrial uncoupler FCCP. The maximal respiration was significantly increased following treatment with Alda-1 (Fig. 4E). These changes suggested that treatment with Alda-1 significantly enhanced the mitochondrial respiration.

The OCR is an indicator of oxidative phosphorylation (OXPHOS), a process that is responsible for ATP production in mitochondria [34]. ATP production was analyzed in ORSCs post-treatment with Alda-1. The results demonstrated that Alda-1 treatment led to a significant elevation in ATP formation (Fig. 4F). Taken together, these findings indicate that activation of mitochondrial ALDH2 triggers OXPHOS, which increases ATP production.

Activation of ALDH2 activated Akt/GSK3β/β-catenin signaling

Alda-1 administration resulted in the elevation of phospho-Akt, phospho-GSK 3β, and β-catenin levels in ORSCs (Fig. 5A, Supplementary Fig. 3). To identify the proliferation mechanism, we assessed the expression levels of phosphorylated Akt. A significant dose-dependent increase was observed in Akt phosphorylation following treatment with Alda-1. Together with ALDH2 activation in ORSCs, the phosphorylated GSK 3β ratio was elevated. GSK 3β phosphorylation triggers β-catenin degradation with inhibitory serine-phosphorylation. Concurrently, we observed upregulation of total β-catenin, which indicated the accumulation of β-catenin in response to Alda-1 treatment (Fig. 5B). To further confirm the regulation of growth factors by Alda-1 treatment, we employed human growth factor array (Supplementary Fig. 4). The analysis revealed that levels of basic fibroblast growth factor, fibroblast growth factor-7, hepatocyte growth factor, insulin-like growth factor binding protein-1, insulin-like growth factor-1, platelet-derived growth factor (PDGF)-AA, and PDGF-AB were elevated following Alda-1 treatment. Collectively, these findings suggest that ALDH2 activation upregulates β-catenin levels and growth factors, thereby promoting hair growth. Thus, enhancing ALDH2 activity in HFs causes a hair growth-promoting effect.

ALDH2 activation induced anagen in vivo

To investigate whether ALDH2 activation expedites anagen entry *in vivo*, 8 week-old female C57BL/6 mice were subjected to topical treatment with vehicle, 0.5 and 3 mM Alda-1, and Minoxidil as the positive control for 21 days. The 3 mM Alda-1- and Minoxidil-treated groups fully entered the anagen phase on day 21. We observed pigmentation and hair formation on the Alda-1- and Minoxidil-treated mouse skin. Histological sections showed anagen HFs and increased skin thickness in the Alda-1- and Minoxidil-treated groups. Moreover, mice treated with 3 mM Alda-1 and Minoxidil showed observable anagen HFs, whereas the control group treated with the vehicle had telogen HFs. IF staining of DPCs in the Alda-1 and Minoxidil-treated groups showed expression of versican (Fig. 6A), indicating that HFs were in the anagen phase [35]. Additionally, we investigated the expression of β-catenin, an anagen induction marker, through IF staining (Supplementary Fig. 5A, B). The skin thickness was significantly increased in 3 mM Alda-1- and Minoxidil-treated mice (Fig. 6B). Therefore, the anagen induction score, which is based on the morphology of the HFs, in mice receiving Alda-1 treatment was higher than that in mice administered the vehicle. This score was comparable to that observed in mice treated with

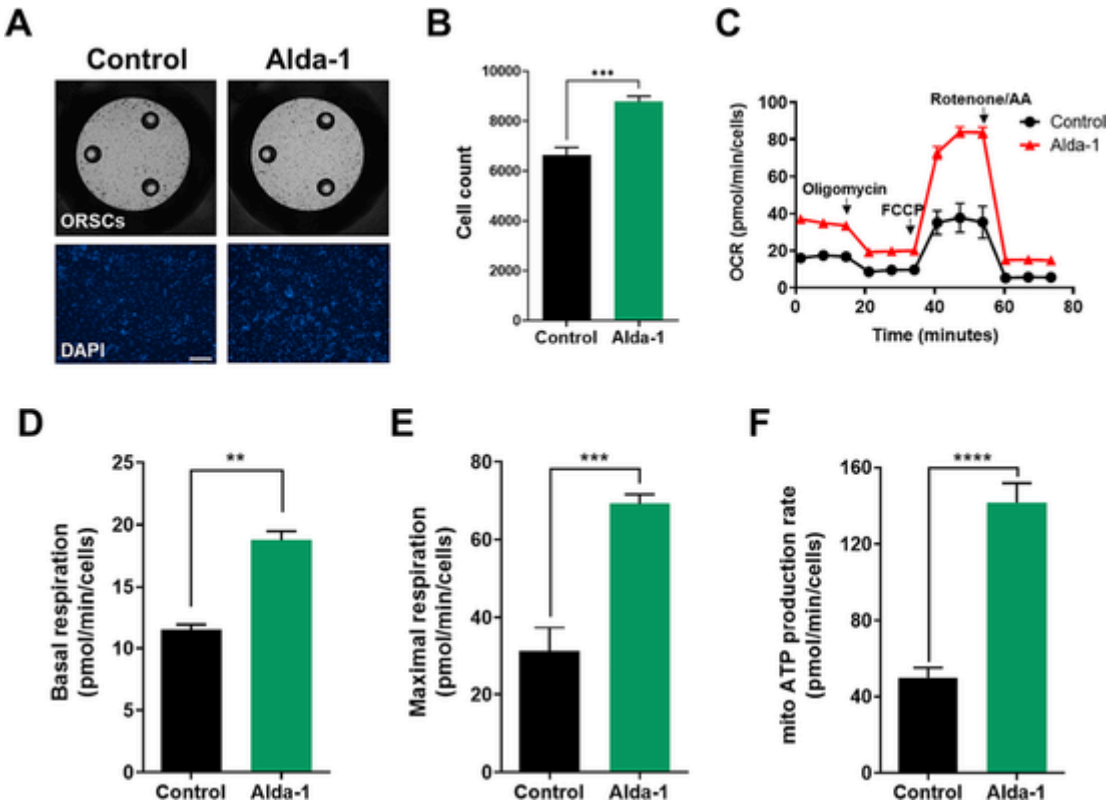

Fig. 4. Activation of ALDH2 enhances mitochondrial oxidative phosphorylation. (A) Confocal images of ORSCs exposed to vehicle and Alda-1; scale bar = 100 μm. (B) Cell count determined using DAPI-positive ORSCs in treated groups. (C) Changes in OCR after treatment with the vehicle and Alda-1. The OCR was normalized to that of the counted cells stained with DAPI. (D) Basal respiration and (E) maximal respiration rates determined using Seahorse Extracellular Flux in both groups. B–E (n = 7/group), **, $P < 0.01$; ***, $P < 0.001$. (F) Quantitative assessment of mitochondrial ATP production revealed a significant enhancement in response to Alda-1 treatment (n = 10/group), ****, $P < 0.0001$. In panels B, D–F, data are presented as mean ± SEM, and statistical analysis was ascertained using an unpaired t-test. ORSCs: outer root sheath cells, DAPI: 4′,6-diamidino-2-phenylindole, FCCP: Carbonyl cyanide 4-(trifluoromethoxy) phenylhydrazone, AA: antimycin A, ALDH2: aldehyde dehydrogenase 2, OCR: oxygen consumption rate, mito ATP: mitochondrial adenosine triphosphate.

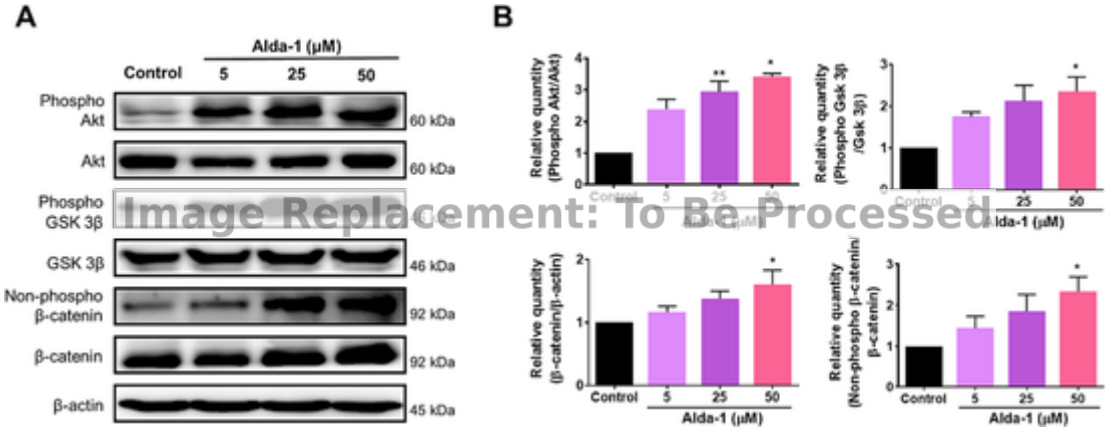

Fig. 5. Upregulation of Akt/GSK 3β/β-catenin signaling in ORSCs as a result of ALDH2 activation. (A) Western blot analysis of Akt/GSK 3β/β-catenin signaling post-treatment with 5, 25, and 50 μM Alda-1. (B) Quantitative analysis to determine the relative levels of phospho-Akt/Akt, phospho-GSK 3β/GSK 3β, β-catenin/β-actin, and non-phospho β-catenin/β-catenin (n = 3 biological replicates/group). Data are presented as mean ± SEM and were analyzed using a one-way ANOVA; *, $P < 0.05$; **, $P < 0.01$. Akt: protein kinase B, GSK: glycogen synthase kinase, ORSCs: outer root sheath cells, ALDH2: aldehyde dehydrogenase 2.

Minoxidil (Fig. 6C). Collectively, these results indicate that Alda-1 treatment effectively induces the anagen hair cycle *in vivo*.

Discussion

ALDH2, an aldehyde dehydrogenase, is known to be a detoxifying enzyme that accumulates through mitochondrial metabolism [36]. Mitochondrial ALDH2 is a ubiquitously expressed enzyme responsible for oxidizing endogenous substances, such as 4-HNE and MDA, which are generated during oxidative degradation of lipids [37]. Dysregulation of ALDH2 is associated with the etiology of numerous human pathologies, including oncological, cardiovascular, musculoskeletal, metabolic, cerebrovascular, dermatological, and senescence-related disorders [32, 38–40]. Among small molecules, Alda-1 is a potent allosteric activator of ALDH2. It exerts its activating effect by binding in proximity to the terminus of the enzyme-substrate binding tunnel, consequently confer-

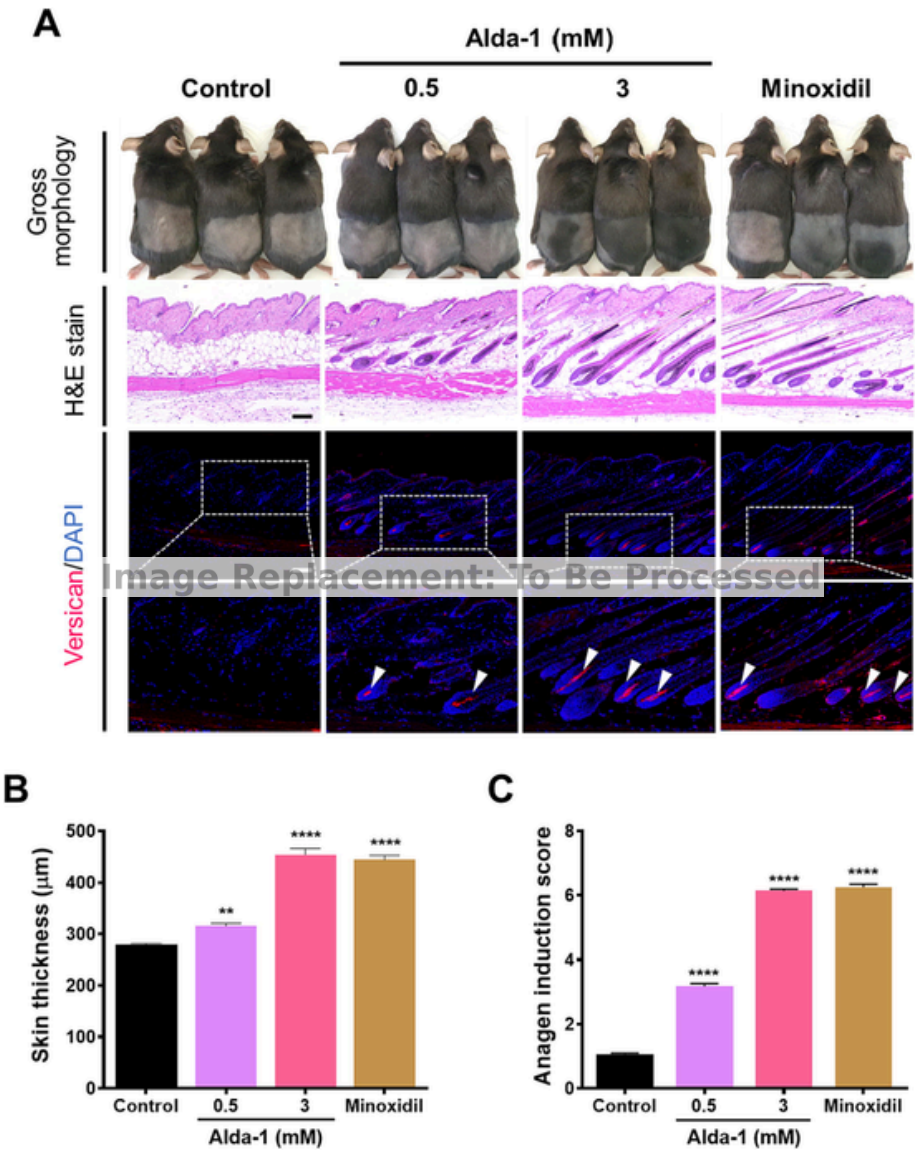

Fig. 6. Topical treatment and activation of ALDH2 induced anagen *in vivo*. (A) Gross morphology, histological sections, and versican immunofluorescence staining indicated anagen induction in groups of mice treated with Alda-1 and 2% Minoxidil, whereas the vehicle-treated group did not show induction; scale bar = 100 μm. (B) Skin thickness increased in the Alda-1- and Minoxidil-treated mice (n = 5/group). **, $P < 0.01$; ****, $P < 0.0001$. (C) The mice treated with Alda-1 and Minoxidil exhibited increased anagen induction scores (n = 70 HFs/group). ****, $P < 0.0001$. For panels B and C, data are presented as mean ± SEM, and statistical significance was determined using a one-way ANOVA. ALDH2: aldehyde dehydrogenase 2, H&E: hematoxylin and eosin, DAPI: 4′,6-diamidino-2-phenylindole, HF: hair follicle.

ring structural stability to the enzyme [41]. The activation mechanism of Alda-1 involves both an increase in the effective concentration of the reactive moieties within the enzyme's catalytic domain and a constraint on substrate diffusion within the enzyme-substrate-binding tunnel following binding events [16,41].

The focus of this investigation was directed towards exploring the effects of ALDH2 on hair growth via scavenging of ROS. Mitochondrial ROS production is more significant in the outermost layer of the HF than in other HF regions, and mitochondrial function is critical for regulating energy metabolism and preventing oxidative stress-induced damage [6,42,43]. The ORS is an epidermal basal layer and an essential region for anagen induction that expresses ATP-binding cassette transporters involved in homeostatic processes, including lipid transport and cell differentiation [44]. Our findings suggest that ALDH2 is predominantly localized within the ORS and functions as a mitochondrial energy supplier in the HF. Despite the fact that glycolysis is the primary energy source in HFs [45–48], our investigation unveiled a multifaceted role of ALDH2, encompassing not only participation in glycolysis but also engagement in OXPHOS-mediated ATP production (Supplementary Fig. 6). However, further investigations are required to elucidate the mechanism by which the mitochondrial enzyme ALDH2 functions during the hair cycle.

Oxidative stress generates a range of reactive intermediates that surpass the capacity of the antioxidant defense system, resulting in cellular damage [13]. During ROS bursts, highly active lipid peroxidation byproducts are produced [19]. Free radicals are involved in the pathogenesis of hair loss [15]; hence, redox imbalance and mitochondrial enzyme dysregulation in plasma cause skin and hair disorders [11]. Moreover, oxidative stress induces premature catagen entry and causes hair loss [13,49,50]. This multifaceted process is further nuanced by the elevation in ROS levels, which acts as a catalyst for lipid peroxidation. This cascade culminates in the production of highly reactive aldehydes such as 4-HNE and MDA. The precise cellular implications of these adducts remain partially characterized, yet the propensity to engage with pro-

teins and generate cytotoxic adducts is recognized as a disruptive mechanism within cells [51]. A recent study uncovered a correlation between the elevation of 4-HNE levels and ROS production within human HFs [13]. Although our study did not investigate this aspect, the exploration of direct interactions between these reactive aldehydes and HFs, including the mechanisms through which they may induce the catagen phase, represents an intriguing direction for future research. ALDH2-mediated clearance of 4-HNE provides protection against oxidative stress-associated diseases, including stroke and alcoholic liver disease [33,52]. Our findings indicate that ALDH2 activation promotes the anagen phase by removing excessive ROS and harmful adducts. Furthermore, Alda-1 treatment induced the anagen phase by reducing excessive ROS and harmful adducts in HFs. This is in agreement with the results of previous studies showing that ALDH2 activation by an activator diminishes ROS production, which increases hair stem cell proliferation and inhibits hair regeneration [53].

We also investigated the effect of Alda-1 on HF growth through Akt/GSK-3β/β-catenin signaling. Akt promotes cell proliferation, and its activity is regulated by phosphorylation [54]. Our findings revealed that Alda-1 treatment resulted in Akt phosphorylation in ORSCs, subsequently leading to GSK 3β phosphorylation. GSK 3β initiates β-catenin degradation through phosphorylation of specific serine and threonine residues, leading to its recognition by the ubiquitin–proteasome system for subsequent proteolysis. Moreover, GSK 3β inhibition prevents β-catenin degradation. The morphology and development of HFs depend on several signaling pathways. There is a notable upregulation of Akt and Wnt/β-catenin signaling pathways in human ORSCs during cellular proliferation [21,55]. One potential strategy for promoting entry into the anagen stage and treating hair loss is to increase the intracellular accumulation of β-catenin. Experimental evidence suggests that β-catenin is vital for HF formation, maintenance, morphogenesis, and cycling, with its deletion resulting in hair loss following the first hair cycle [56,57]. This observation suggests a possible mechanism underlying the promotion of hair growth by ALDH2 activation, highlighting its potential as a therapeutic avenue for the induction of anagen. The participation of numerous paracrine components in β-catenin signaling underscores their critical role in the promotion and preservation of hair growth, emphasizing the molecular complexity of HFs [58,59]. Further investigations are required to clarify how ROS-mediated activation of ALDH2 affects the signaling pathways involved in hair growth. In the current study, we used Alda-1 as an ALDH2 activator that efficiently scavenges aldehyde adducts. Future research will be focused on the intermediate mechanisms involved in oxidative stress and β-catenin modulation by ALDH2 in HFs.

Several studies have reported the genetic factors associated with hair loss [2,3,60]. A recent study revealed that *PPARGC1A* and *ABCC4* are essential genes involved in early onset female pattern hair loss (eFPHL) and regulate mitochondrial biogenesis related to ATP stimulation. In addition, two single nucleotide polymorphisms (SNPs) related to ALDH2 (rs59154828 and rs16941669) have been reported to be associated with eFPHL [3]. SNPs are useful for tracking the inheritance of disease-related genetic modifications and predicting the risk of developing certain diseases or drug responses in individuals [61]. This study explored the potential of ALDH2 activation in promoting hair growth and revealed that ALDH2 activation in HFs induces anagen. These findings indicate that ALDH2 is a potential pharmacological target, thereby signifying a promising direction for therapeutic interventions in the induction of anagen.

Conclusion

This study explored the effects of ALDH2 activation on hair growth. Our findings demonstrated that ALDH2 activation alleviates oxidative stress via 4-HNE and MDA in ORSCs. Further experiments demonstrated that ALDH2 activation triggers β-catenin accumulation and subsequently induces anagen. These findings indicate that ALDH2 activation could potentially represent a promising strategy for inducing anagen.

Compliance with ethics requirements

The human study was approved by the Institutional Review Board of Seoul National University Hospital (2209-021-1356) and followed ethical guidelines. Animal research was approved by the Institutional Animal Care and Use Committee of Seoul National University Hospital (20-0166-S1A1).

CRediT authorship contribution statement

Seunghee Lee : Conceptualization, Investigation, Data curation, Formal analysis, Writing - original draft, Writing - review & editing. **Jungyoon Ohn :** Conceptualization, Investigation, Data curation. **Bo Mi Kang :** Investigation, Formal analysis. **Sungjoo Tommy Hwang :** Investigation. **Ohsang Kwon :** Supervision, Conceptualization, Formal analysis, Writing - review & editing.

Declaration of Competing Interest

The authors declare that they have no known competing financial interests or personal relationships that could have appeared to influence the work reported in this paper.

Acknowledgements

This work was supported by the Seoul National University Hospital Research Fund (No. 03-2021-0010), and by a grant of the Korea Health Technology R&D Project through the Korea Health industry Development institute (KHIDI), funded by the Ministry of Health and Welfare, Republic or Korea (Grant number: HP23C0102).

Appendix A. Supplementary data

Supplementary data to this article can be found online at https://doi.org/10.1016/j.jare.2023.11.014.

References

[1] Adil A, Godwin M. The effectiveness of treatments for androgenetic alopecia: A systematic review and meta-analysis. J Am Acad Dermatol 2017;77:136–41. https://doi.org/10.1016/j.jaad.2017.02.054.
[2] Happle R. Genetic hair loss. Clin Dermatol 2001;19:121–8. https://doi.org/10.1016/S0738-081X(00)00122-X.
[3] Ohn J, Son H.Y, Yu D.A, Kim M.S, Kwon S, Park W.S, et al. Early onset female pattern hair loss: A case-control study for analyzing clinical features and genetic variants. J Dermatol Sci 2022;106:21–8. https://doi.org/10.1016/j.jdermsci.2022.02.011.
[4] Müller-Röver S, Handjiski B, van der Veen C, Eichmüller S, Foitzik K, McKay I.A, et al. A comprehensive guide for the accurate classification of murine hair follicles in distinct hair cycle stages. J Invest Dermatol 2001;117:3–15. https://doi.org/10.1046/j.0022-202x.2001.01377.x.
[5] Vidali S, Knuever J, Lerchner J, Giesen M, Bíró T, Klinger M, et al. Hypothalamic-pituitary-thyroid axis hormones stimulate mitochondrial function and biogenesis in human hair follicles. J Invest Dermatol 2014;134:33–42. https://doi.org/10.1038/jid.2013.286.
[6] Lemasters J.J, Ramshesh V.K, Lovelace G.L, Lim J, Wright G.D, Harland D, et al. Compartmentation of mitochondrial and oxidative metabolism in growing hair follicles: A ring of fire. J Invest Dermatol 2017;137:1434–44. https://doi.org/10.1016/j.jid.2017.02.983.
[7] Paus R, Cotsarelis G. The biology of hair follicles. N Engl J Med 1999;341:491–7. https://doi.org/10.1056/NEJM199908123410706.
[8] Geyfman M, Plikus M.V, Treffeisen E, Andersen B, Paus R. Resting no more: re-defining telogen, the maintenance stage of the hair growth cycle. Biol Rev Camb Philos Soc 2015;90:1179–96. https://doi.org/10.1111/brv.12151.
[9] Myung P, Ito M. Dissecting the bulge in hair regeneration. J Clin Invest 2012;122:448–54. https://doi.org/10.1172/JCI57414.
[10] Choi Y.S, Zhang Y, Xu M, Yang Y, Ito M, Peng T, et al. Distinct functions for Wnt/beta-catenin in hair follicle stem cell proliferation and survival and interfollicular epidermal homeostasis. Cell Stem Cell 2013;13:720–33. https://doi.org/10.1016/j.stem.2013.10.003.
[11] Bodemer C, Rötig A, Rustin P, Cormier V, Niaudet P, Saudubray J.M, et al. Hair and skin disorders as signs of mitochondrial disease. Pediatrics 1999;103:428–33. https://doi.org/10.1542/peds.103.2.428.

[12] Ohn J, Kim S.J, Choi S.J, Choe Y.S, Kwon O, Kim K.H. Hydrogen peroxide (H2O2) suppresses hair growth through downregulation of beta-catenin. J Dermatol Sci 2018;89:91–4. https://doi.org/10.1016/j.jdermsci.2017.09.003.

[13] Haslam I.S, Jadkauskaite L, Szabó I.L, Staege S, Hesebeck-Brinckmann J, Jenkins G, et al. Oxidative damage control in a human (mini-) organ: Nrf2 activation protects against oxidative stress-induced hair growth inhibition. J Invest Dermatol 2017;137:295–304. https://doi.org/10.1016/j.jid.2016.08.035.

[14] Upton J.H, Hannen R.F, Bahta A.W, Farjo N, Farjo B, Philpott M.P. Oxidative stress-associated senescence in dermal papilla cells of men with androgenetic alopecia. J Invest Dermatol 2015;135:1244–52. https://doi.org/10.1038/jid.2015.28.

[15] Trüeb R.M, Henry J.P, Davis M.G, Schwartz J.R. Scalp condition impacts hair growth and retention via oxidative stress. Int J Trichology 2018;10:262–70. https://doi.org/10.4103/ijt.ijt_57_18.

[16] Gao J, Hao Y, Piao X, Gu X. Aldehyde dehydrogenase 2 as a therapeutic target in oxidative stress-related diseases: post-translational modifications deserve more attention. Int J Mol Sci 2022;23. https://doi.org/10.3390/ijms23052682.

[17] Balber A.E. Concise review: aldehyde dehydrogenase bright stem and progenitor cell populations from normal tissues: characteristics, activities, and emerging uses in regenerative medicine. Stem Cells 2011;29:570–5. https://doi.org/10.1002/stem.613.

[18] Chen C.H, Budas G.R, Churchill E.N, Disatnik M.H, Hurley T.D, Mochly-Rosen D. Activation of aldehyde dehydrogenase-2 reduces ischemic damage to the heart. Science 2008;321:1493–5. https://doi.org/10.1126/science.1158554.

[19] Zhang T, Zhao Q, Ye F, Huang C.Y, Chen W.M, Huang W.Q. Alda-1, an ALDH2 activator, protects against hepatic ischemia/reperfusion injury in rats via inhibition of oxidative stress. Free Radic Res 2018;52:629–38. https://doi.org/10.1080/10715762.2018.1459042.

[20] Limat A, Noser F.K. Serial cultivation of single keratinocytes from the outer root sheath of human scalp hair follicles. J Invest Dermatol 1986;87:485–8. https://doi.org/10.1111/1523-1747.ep12455548.

[21] Zhang H, Nan W, Wang S, Zhang T, Si H, Yang F, et al. Epidermal growth factor promotes proliferation and migration of follicular outer root sheath cells via Wnt/beta-catenin signaling. Cell Physiol Biochem 2016;39:360–70. https://doi.org/10.1159/000445630.

[22] Ohn J, Been K.W, Kim J.Y, Kim E.J, Park T, Yoon H.J, et al. Discovery of a transdermally deliverable pentapeptide for activating AdipoR1 to promote hair growth. EMBO Mol Med 2021;13:e13790. https://doi.org/10.15252/emmm.202013790.

[23] Limat A, Hunziker T, Boillat C, Bayreuther K, Noser F. Post-mitotic human dermal fibroblasts efficiently support the growth of human follicular keratinocytes. J Invest Dermatol 1989;92:758–62. https://doi.org/10.1111/1523-1747.ep12722530.

[24] Jo S.J, Choi S.J, Yoon S.Y, Lee J.Y, Park W.S, Park P.J, et al. Valproic acid promotes human hair growth in in vitro culture model. J Dermatol Sci 2013;72:16–24. https://doi.org/10.1016/j.jdermsci.2013.05.007.

[25] Messenger A.G. The culture of dermal papilla cells from human hair follicles. Br J Dermatol 1984;110:685–9. https://doi.org/10.1111/j.1365-2133.1984.tb04705.x.

[26] Kloepper J.E, Sugawara K, Al-Nuaimi Y, Gáspár E, van Beek N, Paus R. Methods in hair research: how to objectively distinguish between anagen and catagen in human hair follicle organ culture. Exp Dermatol 2010;19:305–12. https://doi.org/10.1111/j.1600-0625.2009.00939.x.

[27] Kwon O.S, Oh J.K, Kim M.H, Park S.H, Pyo H.K, Kim K.H, et al. Human hair growth ex vivo is correlated with in vivo hair growth: selective categorization of hair follicles for more reliable hair follicle organ culture. Arch Dermatol Res 2006;297:367–71. https://doi.org/10.1007/s00403-005-0619-z.

[28] Plitzko B, Loesgen S. Measurement of oxygen consumption rate (OCR) and extracellular acidification rate (ECAR) in culture cells for assessment of the energy metabolism. Bio Protoc 2018;8:e2850.

[29] Choi H.I, Kim D.Y, Choi S.J, Shin C.Y, Hwang S.T, Kim K.H, et al. The effect of cilostazol, a phosphodiesterase 3 (PDE3) inhibitor, on human hair growth with the dual promoting mechanisms. J Dermatol Sci 2018;91:60–8. https://doi.org/10.1016/j.jdermsci.2018.04.005.

[30] Buffoli B, Rinaldi F, Labanca M, Sorbellini E, Trink A, Guanziroli E, et al. The human hair: from anatomy to physiology. Int J Dermatol 2014;53:331–41. https://doi.org/10.1111/ijd.12362.

[31] Eruslanov E, Kusmartsev S. Identification of ROS using oxidized DCFDA and flow-cytometry. Methods Mol Biol 2010;594:57–72. https://doi.org/10.1007/978-1-60761-411-1_4.

[32] Guo J.M, Liu A.J, Zang P, Dong W.Z, Ying L, Wang W, et al. ALDH2 protects against stroke by clearing 4-HNE. Cell Res 2013;23:915–30. https://doi.org/10.1038/cr.2013.69.

[33] Ma H, Guo R, Yu L, Zhang Y, Ren J. Aldehyde dehydrogenase 2 (ALDH2) rescues myocardial ischaemia/reperfusion injury: role of autophagy paradox and toxic aldehyde. Eur Heart J 2011;32:1025–38. https://doi.org/10.1093/eurheartj/ehq253.

[34] Sun X, Gao R, Li W, Zhao Y, Yang H, Chen H, et al. Alda-1 treatment promotes the therapeutic effect of mitochondrial transplantation for myocardial ischemia-reperfusion injury. Bioact Mater 2021;6:2058–69. https://doi.org/10.1016/j.bioactmat.2020.12.024.

[35] Soma T, Tajima M, Kishimoto J. Hair cycle-specific expression of versican in human hair follicles. J Dermatol Sci 2005;39:147–54. https://doi.org/10.1016/j.jdermsci.2005.03.010.

[36] Chen C.H, Ferreira J.C, Gross E.R, Mochly-Rosen D. Targeting aldehyde dehydrogenase 2: New therapeutic opportunities. Physiol Rev 2014;94:1–34. https://doi.org/10.1152/physrev.00017.2013.

[37] Zhao Y, Wang B, Zhang J, He D, Zhang Q, Pan C, et al. ALDH2 (aldehyde dehydrogenase 2) protects against hypoxia-induced pulmonary hypertension. Arterioscler Thromb Vasc Biol 2019;39:2303–19. https://doi.org/10.1161/ATVBAHA.119.312946.

[38] Zhang H, Fu L. The role of ALDH2 in tumorigenesis and tumor progression: targeting ALDH2 as a potential cancer treatment. Acta Pharm Sin B 2021;11:1400–11. https://doi.org/10.1016/j.apsb.2021.02.008.

[39] Chen Y.C, Lu R.B, Peng G.S, Wang M.F, Wang H.K, Ko H.C, et al. Alcohol metabolism and cardiovascular response in an alcoholic patient homozygous for the ALDH2*2 variant gene allele. Alcohol Clin Exp Res 1999;23:1853–60. https://doi.org/10.1111/j.1530-0277.1999.tb04083.x. PMID: 10630602.

[40] Zhang Y, Babcock S.A, Hu N, Maris J.R, Wang H, Ren J. Mitochondrial aldehyde dehydrogenase (ALDH2) protects against streptozotocin-induced diabetic cardiomyopathy: role of GSK3beta and mitochondrial function. BMC Med 2012;10:40. https://doi.org/10.1186/1741-7015-10-40.

[41] Perez-Miller S, Younus H, Vanam R, Chen C.H, Mochly-Rosen D, Hurley T.D. Alda-1 is an agonist and chemical chaperone for the common human aldehyde dehydrogenase 2 variant. Nat Struct Mol Biol 2010;17:159–64. https://doi.org/10.1038/nsmb.1737.

[42] Parker G.C, Acsadi G, Brenner C.A. Mitochondria: determinants of stem cell fate? Stem Cells Dev 2009;18:803–6. https://doi.org/10.1089/scd.2009.1806.edi.

[43] Hamanaka R.B, Chandel N.S. Mitochondrial metabolism as a regulator of keratinocyte differentiation. Cell Logist 2013;3:e25456.

[44] Haslam I.S, El-Chami C, Faruqi H, Shahmalak A, O'Neill C.A, Paus R. Differential expression and functionality of ATP-binding cassette transporters in the human hair follicle. Br J Dermatol 2015;172:1562–72. https://doi.org/10.1111/bjd.13549.

[45] Williams R, Philpott M.P, Kealey T. Metabolism of freshly isolated human hair follicles capable of hair elongation: a glutaminolytic, aerobic glycolytic tissue. J Invest Dermatol 1993;100:834–40. https://doi.org/10.1111/1523-1747.ep12476744.

[46] Flores A, Schell J, Krall A.S, Jelinek D, Miranda M, Grigorian M, et al. Lactate dehydrogenase activity drives hair follicle stem cell activation. Nat Cell Biol 2017;19:1017–26. https://doi.org/10.1038/ncb3575.

[47] Miranda M, Christofk H, Jones D.L, Lowry W.E. Topical inhibition of the electron transport chain can stimulate the hair cycle. J Invest Dermatol 2018;138:968–72. https://doi.org/10.1016/j.jid.2017.10.021.

[48] Flores A, Choi S, Hsu Y.C, Lowry W.E. Inhibition of pyruvate oxidation as a versatile stimulator of the hair cycle in models of alopecia. Exp Dermatol 2021;30:448–56. https://doi.org/10.1111/exd.14307.

[49] Paus R, Haslam I.S, Sharov A.A, Botchkarev V.A. Pathobiology of chemotherapy-induced hair loss. Lancet Oncol 2013;14:e50–9. https://doi.org/10.1016/S1470-2045(12)70553-3.

[50] Foitzik K, Spexard T, Nakamura M, Halsner U, Paus R. Towards dissecting the pathogenesis of retinoid-induced hair loss: all-trans retinoic acid induces premature hair follicle regression (catagen) by upregulation of transforming growth factor-beta2 in the dermal papilla. J Invest Dermatol 2005;124:1119–26. https://doi.org/10.1111/j.0022-202X.2005.23686.x.

[51] Ning S, Budas G.R, Churchill E.N, Chen C.H, Knox S.J, Mochly-Rosen D. Mitigation of radiation-induced dermatitis by activation of aldehyde dehydrogenase 2 using topical alda-1 in mice. Radiat Res 2012;178:69–74. https://doi.org/10.1667/rr2861.1.

[52] Shoeb M, Ansari N.H, Srivastava S.K, Ramana K.V. 4-hydroxynonenal in the pathogenesis and progression of human diseases. Curr Med Chem 2014;21:230–7. https://doi.org/10.2174/09298673113209990181.

[53] Tang Y, Luo B, Deng Z, Wang B, Liu F, Li J, et al. Mitochondrial aerobic respiration is activated during hair follicle stem cell differentiation, and its dysfunction retards hair regeneration. PeerJ 2016;4:e1821.

[54] Manning B.D, Toker A. AKT/PKB Signaling: Navigating the Network. Cell 2017;169:381–405. https://doi.org/10.1016/j.cell.2017.04.001.

[55] Lee Y.J, Park S.H, Park H.R, Lee Y, Kang H, Kim J.E. Mesenchymal stem cells antagonize IFN-induced proinflammatory changes and growth inhibition effects via Wnt/beta-catenin and JAK/STAT pathway in human outer root sheath cells and hair follicles. Int J Mol Sci 2021;22. https://doi.org/10.3390/ijms22094581.

[56] Huelsken J, Vogel R, Erdmann B, Cotsarelis G, Birchmeier W. Beta-catenin controls hair follicle morphogenesis and stem cell differentiation in the skin. Cell 2001;105:533–45. https://doi.org/10.1016/s0092-8674(01)00336-1.

[57] Collins C.A, Kretzschmar K, Watt F.M. Reprogramming adult dermis to a neonatal state through epidermal activation of beta-catenin. Development 2011;138:5189–99. https://doi.org/10.1242/dev.064592.

[58] Premanand A, Reena R.B. Androgen modulation of Wnt/beta-catenin signaling in androgenetic alopecia. Arch Dermatol Res 2018;310:391–9. https://doi.org/10.1007/s00403-018-1826-8.

[59] Botchkarev V.A, Kishimoto J. Molecular control of epithelial-mesenchymal interactions during hair follicle cycling. J Investig Dermatol Symp Proc 2003;8:46–55. https://doi.org/10.1046/j.1523-1747.2003.12171.x.

[60] Redler S, Brockschmidt F.F, Tazi-Ahnini R, Drichel D, Birch M.P, Dobson K, et al. Investigation of the male pattern baldness major genetic susceptibility loci AR/EDA2R and 20p11 in female pattern hair loss. Br J Dermatol 2012;166:1314–8. https://doi.org/10.1111/j.1365-2133.2012.10877.x.

[61] Shastry B.S. SNPs in disease gene mapping, medicinal drug development and evolution. J Hum Genet 2007;52:871–80. https://doi.org/10.1007/s10038-007-0200-z.